



Fractional-Order Dynamics and Fear-Induced Bifurcation in Delayed Food Chain Model

Vinoth Seralan *

*Center for Nonlinear and Complex Networks,
SRM Institute of Science and Technology,
Ramapuram, Chennai 600089, Tamil Nadu, India
svinothappu@gmail.com*

R. Vadivel *

*Department of Mathematics, Phuket Rajabhat University,
Faculty of Science and Technology, Phuket 83000, Thailand
vadivelsr@yahoo.com*

Nallappan Gunasekaran

*Eastern Michigan Joint College of Engineering,
Beibu Gulf University, Qinzhou 535011, P. R. China
gunasmaths@gmail.com*

Received March 29, 2024; Accepted August 20, 2024; Published April 7, 2025

This paper investigates the bifurcation problem in a fractional-order delayed food chain model that incorporates a fear effect. We observe that the fractional order significantly impacts the delayed system, influencing its stability in the presence of fear. Both the fractional order and the fear effect play crucial roles in determining the system's stability. Furthermore, we observe stability switching induced by the fear effect while keeping the delay fixed. We identify the stability condition of the proposed model and precisely establish bifurcation points by utilizing delay as a bifurcation parameter. The system exhibits robust stability performance with smaller control parameters, and Hopf bifurcation arises as the control parameter surpasses a critical value. Additionally, through theoretical analysis and numerical simulations, we investigate the effects of fractional order, the fear effect, and time delay on the system's stability.

Keywords: Fractional order; time delay; stability; Hopf bifurcation; food chain model.

1. Introduction

The mathematical representation of predator–prey dynamics is a cornerstone in theoretical ecology and biomathematics, reflecting the intricate interplay between species in ecosystems [Brauer & Castillo-Chavez, 2012; Britton, 2003]. This relationship not only underpins the structure of food chains, webs, and biochemical networks but also serves as a vital tool for understanding population dynamics,

disease outbreaks, and control strategies [Hethcote, 2000; Neuhauser, 2001]. Researchers have extensively studied the impact of fear within predator–prey models in recent literature, exploring its effects on population dynamics and stability [Vinoth *et al.*, 2021b; Vinoth *et al.*, 2023; Kumbhakar *et al.*, 2024]. The prey reproduction process is affected by direct predation and also, due to the behavior and physiology of prey. These forms of behavioral and

*Authors for correspondence

physiological modification are related to the fear of prey by its predators, and it is long-lasting compared to direct predation. For instance, wolves in the Greater Yellowstone Ecosystem have an impact on elks' reproductive physiology [Creel *et al.*, 2007]. Additionally, the scared prey species instinctively forage less, which slows their growth rate and forces them to fall back to survival strategies like hunger. Birds have anti-predator defenses in response to the sound of predators [Creel *et al.*, 2007; Cresswell, 2011]. Further, Kumar and Kumari [2020] delved into the influence of multiple fear effects within food chain models, uncovering a range of complex dynamics resulting from the presence or absence of fear.

In nature, the effect of one species on another is not always immediate. For instance, the prey is not immediately available after birth; it takes time to mature (maturation delay). Additionally, when a predator eats prey, the conversion of energy and its influence on the increase of predator population take time (gestation delay) [Vinoth *et al.*, 2021a; Dubey & Kumar, 2019]. Prey-predator models with time delays have seen a substantial increase in interest during the last three decades, primarily due to their propensity to induce bifurcation phenomena and facilitate multiple stability-switching behaviors. A compelling example of this lies in the stability and Hopf bifurcation analysis conducted on stage-structured prey-predator models with gestation delays, as demonstrated by [Bandyopadhyay & Banerjee, 2006]. Furthermore, Upadhyay and Agrawal [2016] introduced gestation time lag into a predator-prey model featuring a generalized predator, alongside incorporating the interaction term in the Beddington-DeAngelis functional form. Their findings revealed that the model under consideration exhibited Hopf bifurcation, particularly for larger values of time delay, with stability analysis facilitated through the center manifold theorem. Similar investigations into the dynamics of predator-prey systems under time delay conditions have been undertaken in other studies [Xiao & Chen, 2001; Xu, 2011; Kuang, 1993; Islam *et al.*, 2023]. Consequently, delving into the impact of time delays on these models is crucial for accurately capturing their dynamical properties, given their reliance on past system information. Many of these investigations have centered around examining the existence and stability of equilibrium points within integer-order predator-prey models.

In natural ecosystems, prey species often require time to assess the risk of predation after detecting chemical or vocal cues [Ripple & Beschta, 2004; Pal *et al.*, 2019; Laundré *et al.*, 2001; Pal *et al.*, 2024]. Unlike immediate reactions, this assessment process involves a delay before the prey's fear of predation affects its behavior. Therefore, it is essential to modify the predator-prey model to accommodate this fear response delay. This adjustment acknowledges the temporal dynamics inherent in predator-prey interactions, where the fear response of prey species evolves gradually over time rather than immediately impacting population dynamics [Panday *et al.*, 2020]. By incorporating this delay, we aim to depict the nuanced dynamics of predator-prey relationships more accurately, reflecting the complex interplay between perception, assessment, and response to predation risk in natural ecosystems.

Fractional calculus is a widely used technique in many different domains, including neural networks, illness treatment, and optimum design. It has proven to be particularly effective in characterizing the memory and heredity features of different materials and processes [Laskin, 2000; Fan *et al.*, 2018; Naik *et al.*, 2020]. Elsadany and Matouk [2015] earlier highlighted the close relationship between fractional-order differential equations and fractals. Natural systems with memory, which are found in the majority of biological systems, are connected to fractional-order equations [Du *et al.*, 2013]. Furthermore, fractals, which are abundant in biological systems, are strongly connected to them. Fractional-time-order derivatives have been shown to have enormous relevance in practical mathematics in recent years [Rasooli Berardehi *et al.*, 2023; Taheri *et al.*, 2023; Roohi *et al.*, 2023a]. With time delays, fractional-order predator-prey models have gained substantial interest from researchers in recent years, and several important results have been made in this area. In an effort to contribute to the expanding research in this field, Zhao *et al.* [2021] examined the effects of numerous time delays in a fractional-order predator model. The study of synchronization of fractional-order neural networks with time delay using dynamic-free adaptive sliding mode control has been investigated by [Roohi *et al.*, 2023b]. Furthermore, some recent literature studies about similar usage of the problems of fractional-order dynamics and about Caputo-type fractional-order derivatives for similar scientific problem can

be found in multiple works such as [Wang *et al.*, 2022; Al-Raei, 2021; Sabarathinam *et al.*, 2023]. This trend underscores the recognition of fractional calculus as a valuable framework for understanding complex dynamics in ecological systems, offering insights that extend beyond traditional integer-order models.

In [Panja, 2019; Das & Samanta, 2020; Ali-dousti & Mostafavi Ghahfarokhi, 2019; Qi & Zhao, 2022; Cui & Zhao, 2024; Huang *et al.*, 2023], limited research has been dedicated to exploring the dynamics of delayed fractional-order food chain models incorporating fear and time delay. In this study, we extend the investigation to incorporate fractional order and time delay into an integer-order food chain model previously examined by [Kumar & Kumari, 2020]. The existing literature lacks precision regarding the dynamics of such systems. It is more realistic to analyze the dynamics of delayed food-chain model with time delay, considering the innate biological distinctions between prey and predator populations. Specifically, there is still much to learn about bifurcation events in fractional-order predator-prey systems with temporal delays. Therefore, studying the dynamic behaviors of fractional-order systems with different delays is essential. The time delay considered in our study is similar to that of delay considered in the model in [Panday *et al.*, 2020]. In the following ways, our model differs from the model examined in earlier research. The chaotic food chain model describes the interaction of prey, specialist predators and top specialist predators studied by [Rai & Upadhyay, 2004]. Kumar and Kumari [2020] extended the model studied by [Rai & Upadhyay, 2004] in the presence of fear effect in both prey and specialist predators. The predator-prey model with fear in the prey growth term and time delay in the fear term have been explored in [Panday *et al.*, 2020]. The predator prey model consists of immature and mature predators with time delay studied by [Huang *et al.*, 2018]. They considered feedback time delay and time delay in virtue of the gestation of the mature predator.

Motivated by these considerations, we extended the model studied in [Kumar & Kumari, 2020] with time delay similar to that of in [Panday *et al.*, 2020] and explored stability, bifurcation in the fractional-order dynamics. This work's main contributions are summed up as follows: (1) Examining bifurcation phenomena in a fractional-order food chain model

that takes fear into account. (2) Using time delay as a bifurcation parameter, deriving bifurcation conditions. (3) Putting forward a framework for the investigation of two fear effects with time delay in the fractional-order food chain model.

This paper is arranged as follows. Section 2 presents definitions and the construction of the model. The stability analysis of all potential equilibrium points is discussed in Sec. 3. Section 4 investigates the conditions for the existence of Hopf bifurcation in the fractional-order delayed food chain model. Numerical examples illustrating the intricate dynamics of the model are given in Sec. 5. Finally, Sec. 6 concludes by highlighting the ecological significance of the analytical findings.

2. Preliminaries

This section introduces fundamental definitions and establishes the formulation of the fractional-order delayed food chain model considered in our study.

Definition 2.1. The Caputo fractional-order derivative is given by

$$D^\alpha f(t) = \frac{1}{\Gamma(\kappa - \alpha)} \int_0^t (t - \lambda)^{\kappa - \alpha - 1} f^{(\kappa)}(\lambda) d\lambda,$$

where $\kappa - 1 < \alpha \leq \kappa \in \mathbb{Z}^+$, $\Gamma(\cdot)$ is the Gamma function. $\Gamma(\lambda) = \int_0^\infty t^{\lambda-1} e^{-t} dt$.

Using Laplace transform, we provide

$$L\{D^\alpha f(t) : \lambda\} = \lambda^\alpha F(\lambda) - \sum_{j=0}^{\kappa-1} \lambda^{\alpha-j-1} f^{(j)}(0),$$

$$\kappa - 1 < \alpha \leq \kappa \in \mathbb{Z}^+.$$

If $f^{(j)} = 0$, $j = 1, 2, \dots, n$, then $L\{D^\alpha f(t); \lambda\} = \lambda^\alpha F(\lambda)$.

Lemma 1. The linear fractional-order systems involving multiple variables are expressed as

$$\left\{ \begin{array}{l} D^{\alpha_1} Y_1(t) = m_{11} Y_1(t) + m_{12} Y_2(t) \\ \quad \quad \quad + \dots + m_{1n} Y_n(t), \\ D^{\alpha_2} Y_2(t) = m_{21} Y_1(t) + m_{22} Y_2(t) \\ \quad \quad \quad + \dots + m_{2n} Y_n(t), \\ \quad \quad \quad \vdots \\ D^{\alpha_n} Y_n(t) = m_{n1} Y_1(t) + m_{n2} Y_2(t) \\ \quad \quad \quad + \dots + m_{nn} Y_n(t), \end{array} \right. \quad (1)$$

where $\alpha_i \in (0, 2]$ ($i = 1, 2, \dots, n$). If α_i is the lowest common multiple of the denominators ξ_j of ϵ_i , where $\alpha_i = \frac{\epsilon_i}{\xi_i}$, $(\epsilon_i, \xi_i) = 1$, $\epsilon_i, \xi_i \in \mathbb{Z}^+$, for $i = 1, 2, \dots, n$. It is given by

$$\Delta(\lambda) = \begin{bmatrix} \lambda^{\alpha_1} - m_{11} & -m_{12} & \cdots & -m_{1n} \\ -m_{21} & \lambda^{\alpha_2} - m_{22} & \cdots & -m_{2n} \\ \vdots & \vdots & \ddots & \vdots \\ -m_{n1} & -m_{n2} & \cdots & \lambda^{\alpha_n} - m_{nn} \end{bmatrix}. \tag{2}$$

Thus, in the Lyapunov sense, if all roots λ of the equation $\det(\Delta(\lambda)) = 0$ satisfy $|\arg(\lambda)| > \alpha_i\pi/2$, then the zero solution of model (1) is globally asymptotically stable.

2.1. Problem formulation

The food chain model, as explored in [Kumar & Kumari, 2020], elucidates the dynamic interplay among prey, middle predators, and top predators, incorporating fear responses in both prey and middle predators. This model is represented as follows:

$$\begin{aligned} \frac{dx}{dt} &= r_0x \frac{1}{1 + \rho_1y} - \delta x - \frac{\beta}{K}x^2 - \frac{a_1xy}{b_1 + x}, \\ \frac{dy}{dt} &= \frac{c_1a_1xy}{b_1 + x} \frac{1}{1 + \rho_2z} - \frac{a_2yz}{b_2 + y} - d_1y, \\ \frac{dz}{dt} &= \frac{c_2a_2yz}{b_2 + y} - d_2z. \end{aligned} \tag{3}$$

Here, x , y , and z denote the populations of prey, middle predators, and top predators at time t , respectively. In the absence of middle and top predators, prey growth follows logistic growth dynamics governed by $\frac{dx}{dt} = rx(1 - \frac{x}{K})$, where $r = r_0 - \delta$ represents the intrinsic growth rate, and r_0 , δ , K , and β denote the growth rate, death rate, carrying capacity of the prey and death rate due to the intraspecific competition, respectively. Conversion rates of prey to predator for species y and z are denoted by c_1 and c_2 , while the death rates for species y and z are represented by d_1 and d_2 , respectively. The terms $\frac{a_1xy}{b_1+x}$ and $\frac{a_2xy}{b_2+x}$ describe the Holling type II interactions between species, where a_i and b_i ($i = 1, 2$) parameterize the saturating functional response. Specifically, b_i represents the prey population level at which the predation rate per unit prey is half of its maximum value. The terms $\frac{1}{1+\rho_1y}$ and $\frac{1}{1+\rho_2z}$ account for fear effects, with ρ_i ($i = 1, 2$)

denoting the strength of fear in prey and middle predators, respectively. For further details regarding the biological assumptions underlying the consideration of fear effects, see Appendix A.

To incorporate fractional-order dynamics, we extend model (3) proposed by [Kumar & Kumari, 2020] by employing Caputo-type fractional-order derivatives instead of normal integer-order derivatives. The resulting model is expressed as

$$\begin{aligned} {}_0^C D_T^{\alpha_1} x &= \frac{r_0x}{1 + \rho_1y(t - \tau)} - \delta x - \frac{\beta}{K}x^2 - \frac{a_1xy}{b_1 + x}, \\ {}_0^C D_T^{\alpha_2} y &= \frac{c_1a_1xy}{b_1 + x} \frac{1}{1 + \rho_2z} - \frac{a_2yz}{b_2 + y} - d_1y, \\ {}_0^C D_T^{\alpha_3} z &= \frac{c_2a_2yz}{b_2 + y} - d_2z. \end{aligned} \tag{4}$$

Here, the initial conditions $x(0) = \psi_1(t) > 0$, $y(0) = \psi_2(t) > 0$, and $z(0) = \psi_3(t) > 0$ are defined for $t \in [-\tau, 0]$, where $\psi(t)$ is a smooth function. The notation ${}_0^C D_t^{\alpha_i}$ (for $i = 1, 2, 3$) represents the Caputo fractional derivative with fractional order α_i ($0 < \alpha_i < 1$). For simplicity, we denote ${}_0^C D_T^{\alpha_i} = D^{\alpha_i}$ and $\sigma = \frac{\beta}{K}$ for further analysis. The parameter τ signifies the time lag involved in prey assessing the risk of predation following the detection of chemical or audio cues, introducing a delayed response between prey population increase and predator threat perception. The model accounts for this delayed cost of fear [Kumar & Kumari, 2020]. The state space of model (4) is constrained to the positive cone $\mathbb{R}_+^3 = (x, y, z) \in \mathbb{R} : x \geq 0, y \geq 0, z \geq 0$.

3. Existence of Equilibria

In this section, we focus on the existence and stability analysis of the interior equilibrium point of model (4). Since, the time delay and fractional order does not influence the number and values of equilibria, the equilibria for model (4) is similar to the model studied in [Kumar & Kumari, 2020], which is calculated by solving the following nonlinear equations:

$$\begin{aligned} \frac{r_0}{1 + \rho_1y^*} - \delta - \sigma x^* - \frac{a_1y^*}{b_1 + x^*} &= 0, \\ \frac{c_1a_1x^*}{b_1 + x^*} \frac{1}{1 + \rho_2z^*} - \frac{a_2z^*}{b_2 + y^*} - d_1 &= 0, \\ \frac{c_2a_2y^*}{b_2 + y^*} - d_2 &= 0. \end{aligned} \tag{5}$$

Let us assume $E^*(x^*, y^*, z^*)$ be the arbitrary coexisting equilibrium points for model (4), which denotes the coexistence of all three species. Here, $y^* = \frac{b_2 d_2}{a_2 c_2 - d_2}$ and x^* is obtained by solving the following equation:

$$\sigma x^{*2} + \left(\sigma b_1 - \frac{r_0}{1 + \rho_1 y^*} + \delta \right) x^* + \left(\delta - \frac{r_0}{1 + \rho_1 y^*} \right) b_1 = 0 \tag{6}$$

and z^* is obtained by solving

$$\frac{a_2 \rho_2}{b + y^*} z^{*2} + \left(\frac{a_2}{b + y^*} + d_1 \rho_2 \right) z^* + \left(d_1 - \frac{c_1 a_1 x^*}{b_1 + x^*} \right) = 0. \tag{7}$$

From the aforementioned equations, it is evident that the following requirements must be met for the coexistence equilibrium point to exist:

$$(H1) \quad a_2 c_2 > d_2, \quad x^* > \frac{d_1 b_1}{c_1 a_1 - d_1},$$

$$\delta < \frac{r_0}{1 + \rho_1 y^*} \quad \text{and} \quad \sigma b_1 + \delta > \frac{r_0}{1 + \rho_1 y^*}.$$

The roots of the equations are difficult to determine analytically, hence in the explanation that follows, we determine numerically in the numerical section.

4. Stability and Hopf Bifurcation

In this section, we deliver the detailed analytical expressions needed to study the stability and Hopf bifurcation analysis for model (4). In an integer-order system, the limit set of a trajectory is a solution; but, in a fractional-order case, it could not be [Tavazoei *et al.*, 2009]. Tavazoei [2010] and Tavazoei and Haeri [2009], respectively, claimed that fractional-order systems do not have periodic orbits and gave an example of a system whose solutions are nonperiodic but converge to periodic signals. According to [Abdelouahab *et al.*, 2012], the Hopf bifurcation produces a limit cycle that draws in nearby solutions rather than being a solution of a fractional system. For similar studies on discussions about periodicity in fractional-order systems, see [Podlubny, 1998; Yazdani & Salarieh, 2011; Danca, 2021]. Similarly, we are concerned with the trajectory's end state in this study, the limit cycle that emerges through a Hopf bifurcation draws in nearby solutions rather than being a solution of a fractional system. The linearized model for model (4)

is obtained by giving a small perturbation to the coexisting equilibrium point E^* and keeping the perturbation variable as same for our convenience. Making use of the transformation $x(t) = x(t) - x^*$, $y(t) = y(t) - y^*$, and $z(t) = z(t) - z^*$, then model (4) becomes

$$\begin{aligned} D^{\alpha_1} x(t) &= p_{11} x(t) + p_{12} y(t) + p_{15} y(t - \tau), \\ D^{\alpha_2} y(t) &= p_{21} x(t) + p_{22} y(t) + p_{23} z(t), \\ D^{\alpha_3} z(t) &= p_{32} y(t), \end{aligned} \tag{8}$$

which is of the form

$$D^{\alpha_i} X = AX(t) + BX(t - \tau), \quad i = 1, 2, 3,$$

where

$$A = \begin{pmatrix} p_{11} & p_{12} & 0 \\ p_{21} & p_{22} & p_{23} \\ 0 & p_{32} & 0 \end{pmatrix}, \quad B = \begin{pmatrix} 0 & p_{15} & 0 \\ 0 & 0 & 0 \\ 0 & 0 & 0 \end{pmatrix}, \tag{9}$$

where

$$\begin{aligned} p_{11} &= -\sigma x^* + \frac{a_1 b_1 y^*}{(b_1 + x^*)^2}, & p_{12} &= -\frac{a_1 x^*}{b_1 + x^*}, \\ p_{15} &= -\frac{r_0 \rho_1 x^*}{(1 + \rho_1 y^*)^2}, & p_{21} &= \frac{a_1 b_1 c_1 y^*}{(b_1 + x^*)^2 (1 + \rho_2 z^*)}, \\ p_{23} &= -\frac{a_2 y^*}{b_2 + y^*} - \frac{a_1 c_1 \rho_2 x^* y^*}{(1 + \rho_2 z^*)^2 (b_1 + x^*)}, \\ p_{22} &= \frac{a_2 y^* z^*}{(b_2 + y^*)^2}, & p_{32} &= \frac{a_2 b_2 c_2 z^*}{(b_2 + y^*)^2}. \end{aligned}$$

Suppose, for the incommensurate fractional-order model (8), the characteristic equation is $\det(\Delta(\lambda)) = 0$, where $\Delta(\lambda) = \lambda^{\alpha_i} I - A - B e^{-\lambda \tau}$.

Therefore, the characteristic equation is given by

$$\det(\lambda^{\alpha_i} I - A - B e^{-\lambda \tau}) = 0, \tag{10}$$

which is difficult to solve since it is a fractional-order equation. The characteristic polynomial is given by

$$M_1(\lambda) + M_2(\lambda) e^{-\lambda \tau} = 0, \tag{11}$$

where

$$\begin{aligned} M_1(\lambda) &= \lambda^{\alpha_1 + \alpha_2 + \alpha_3} - p_{11} \lambda^{\alpha_2 + \alpha_3} - p_{22} \lambda^{\alpha_1 + \alpha_3} \\ &\quad - p_{12} p_{21} \lambda^{\alpha_3} + p_{11} p_{22} \lambda^{\alpha_3} - p_{23} p_{32} \lambda^{\alpha_1} \\ &\quad + p_{11} p_{23} p_{32}, \\ M_2(\lambda) &= -p_{15} p_{21} \lambda^{\alpha_3}. \end{aligned}$$

Let us take $\tau = 0$, Eq. (11) becomes

$$\begin{aligned} &\lambda^{\alpha_1+\alpha_2+\alpha_3} - p_{11}\lambda^{\alpha_2+\alpha_3} - p_{22}\lambda^{\alpha_1+\alpha_3} \\ &- p_{12}p_{21}\lambda^{\alpha_3} - p_{15}p_{21}\lambda^{\alpha_3} + p_{11}p_{22}\lambda^{\alpha_3} \\ &- p_{23}p_{32}\lambda^{\alpha_1} + p_{11}p_{23}p_{32} = 0. \end{aligned}$$

If all the λ_i in (12) obeys $|\arg(\lambda_i)| > \frac{\alpha\pi}{2}$, thus, employing Lemma 1, we can quickly determine that E^* of model (4) is asymptotically stable when $\tau = 0$.

We have the following assumption:

$$(H2) \quad \frac{u_1v_1 + u_2v_2}{v_1^2 + v_2^2} \neq 0,$$

in order to present our main results, where u_1, u_2, v_1, v_2 are described in Eq. (19).

For the commensurate fractional-order, model (4) is considered by taking $\alpha_1 = \alpha_2 = \alpha_3 = \alpha$. Therefore, the characteristic polynomial is given by

$$M_3(\lambda) + M_4(\lambda)e^{-\lambda\tau} = 0, \tag{12}$$

where

$$\begin{aligned} M_1(\lambda) &= \lambda^{3\alpha} - p_{11}\lambda^{2\alpha} - p_{22}\lambda^{2\alpha} - p_{12}p_{21}\lambda^\alpha \\ &+ p_{11}p_{22}\lambda^\alpha - p_{23}p_{32}\lambda^\alpha + p_{11}p_{23}p_{32}, \\ M_2(\lambda) &= -p_{15}p_{21}\lambda^\alpha. \end{aligned}$$

These derivations for finding the characteristic equation are similar to the calculation for all types of three-dimensional fractional-order models with one time delay.

Theorem 1. *Model (4) is asymptotically stable if and only if the real parts of the roots to the characteristic equation (12) are negative.*

Label M_j^r, M_j^i as the real and imaginary parts $M_j(s)(j = 1, 2)$. If $\lambda = \omega(\cos \frac{\pi}{2} + i \sin \frac{\pi}{2})$, $\omega > 0$ is a purely imaginary root of the characteristic equation, then we have

$$\begin{cases} M_2^r \cos \omega\tau + M_2^i \sin \omega\tau = -M_1^r, \\ M_2^i \cos \omega\tau - M_2^r \sin \omega\tau = -M_1^i. \end{cases} \tag{13}$$

From the above equation, we have

$$\begin{cases} \cos \omega\tau = -\frac{g_1(\omega)}{g_3(\omega)}, \\ \sin \omega\tau = -\frac{g_2(\omega)}{g_3(\omega)}, \end{cases}$$

where

$$\begin{aligned} g_1(\omega) &= M_1^r M_2^r + M_1^i M_2^i, \\ g_2(\omega) &= M_1^r M_2^i + M_2^r M_1^i, \\ g_3(\omega) &= (M_2^r)^2 + (M_2^i)^2. \end{aligned}$$

It follows that

$$g_1^2(\omega) + g_2^2(\omega) - g_3^2(\omega) = 0. \tag{14}$$

In terms of $\cos \omega\tau = -\frac{g_1(\omega)}{g_3(\omega)}$, we get

$$\tau_0^{(k)} = \frac{1}{\omega_0} \left[\arccos \left(-\frac{g_1(\omega_0)}{g_3(\omega_0)} \right) + 2k\pi \right], \tag{15}$$

where $k = 0, 1, 2, \dots$, and ω_0 is the positive root of Eq. (14). Define the bifurcation point

$$\tau_0 = \min\{\tau_0^{(k)}\}, \quad k = 0, 1, 2, \dots, \tag{16}$$

where τ_0 is defined earlier.

Similarly, we can prove this for commensurate fractional order.

Lemma 2. *Let $\lambda(\tau) = \xi(\tau) + i\omega_1(\tau)$ be the root of Eq. (11) near $\tau = \tau_j$ satisfying $\xi(\tau_j) = 0$, $\omega(\tau_j) = \omega_0$, then the transversality condition to hold is given as follows:*

$$\Re \left[\frac{d\lambda}{d\tau} \right]_{(\omega=\omega_0, \tau=\tau_0)} \neq 0. \tag{17}$$

Proof. On differentiating Eq. (11), we have

$$\begin{aligned} &U_1'(\lambda) \frac{d\lambda}{d\tau} + U_2'(\lambda) e^{-\lambda\tau} \frac{d\lambda}{d\tau} \\ &+ U_2(\lambda) e^{-\lambda\tau} \left(-\lambda - \tau \frac{d\lambda}{d\tau} \right) = 0. \end{aligned}$$

As a result,

$$\frac{d\lambda}{d\tau} = \frac{u(\lambda)}{v(\lambda)}, \tag{18}$$

where

$$\begin{aligned} u(\lambda) &= \lambda U_2(\lambda) e^{-\lambda\tau}, \\ v(\lambda) &= U_1'(\lambda) + [U_2'(\lambda) - \tau U_2(\lambda)] e^{-\lambda\tau}. \end{aligned}$$

Let u_1, u_2 be the real and imaginary parts of $u(\lambda)$, respectively. v_1, v_2 are the real and imaginary parts of $v(\lambda)$, respectively.

From Eq. (18), we get

$$\Re \left[\frac{d\lambda}{d\tau} \right] \Big|_{(\omega=\omega_0, \tau=\tau_0)} = \frac{u_1v_1 + u_2v_2}{v_1^2 + v_2^2}, \tag{19}$$

where

$$\begin{aligned}
 u_1 &= \omega_0(U_2^r \sin \omega_0 \tau_0 - U_2^i \cos \omega_0 \tau_0), \\
 u_2 &= \omega_0(U_2^r \cos \omega_0 \tau_0 + U_2^i \sin \omega_0 \tau_0), \\
 v_1 &= U_1^r + (U_2^r - \tau_0 U_2^i) \cos \omega_0 \tau_0 \\
 &\quad + (U_2^i - \tau_0 U_2^r) \sin \omega_0 \tau_0, \\
 v_2 &= U_1^i + (U_2^i - \tau_0 U_2^r) \cos \omega_0 \tau_0 \\
 &\quad + (U_2^r - \tau_0 U_2^i) \sin \omega_0 \tau_0. \quad \blacksquare
 \end{aligned}$$

Upon assuming that (H2) holds, then the model (4) satisfies the transversality condition (17). Using Lemmas 1 and 2, we can conclude our results in the following theorem:

Theorem 2. *Using (H1) and (H2), state the following results:*

- If E^* is asymptotically stable for $\tau = 0$, then E^* of the fractional-order model (4) is asymptotically stable when $\tau = [0, \tau_0)$.
- If E^* is asymptotically stable for $\tau = 0$, then model (4) exhibits a Hopf bifurcation near E^* when $\tau = \tau_0$, i.e. the branch of periodic orbits starts emerging from the E^* when $\tau = \tau_0$.

5. Numerical Simulations

In this section, we delve into the exploration of model (4) to substantiate our analytical findings.

All simulations are carried out in Julia software with Predictor–Corrector algorithm for the delayed fractional-order differential equation. We begin by meticulously selecting parameters from [Kumar & Kumari, 2020], which are enumerated as follows:

$$\begin{aligned}
 r_0 &= 2, \quad \rho_1 = 0.1, \quad \rho_2 = 0.1, \\
 \delta &= 0.01, \quad \sigma = 0.05, \\
 a_1 &= 1, \quad b_1 = 10, \quad c_1 = 2, \quad a_2 = 1.5, \\
 b_2 &= 10, \quad d_1 = 1, \quad c_2 = 1, \quad d_2 = 0.7.
 \end{aligned} \tag{20}$$

The initial condition is chosen as (20, 5, 10) for all simulations and step size is taken as 0.01. In the absence of fear parameters ($\rho_1 = 0, \rho_2 = 0$) and under the assumption $\alpha_1 = \alpha_2 = \alpha_3 = 1$, model (4) manifests an interior equilibrium point $E^*(35.9953, 8.75, 7.06466)$. Trajectories around this equilibrium point exhibit chaotic behavior, vividly illustrated in Fig. 1.

Moving forward, by setting a fractional order of $\alpha = 0.9$ and $r_0 = 4$, model (4) converges to an interior equilibrium point $E^*(46.3043, 8.75, 6.75831)$. Nearby trajectories portray asymptotically stable dynamics, particularly under a high strength of fear in prey growth ($\rho_1 = 0.07$), alongside a choice of $\rho_1 = 0.01$ for the middle predator’s fear strength, as evidenced in the time series and phase portrait depicted in Fig. 2. Conversely, for a smaller $\rho_1 = 0.04$, model (4) settles at an interior equilibrium

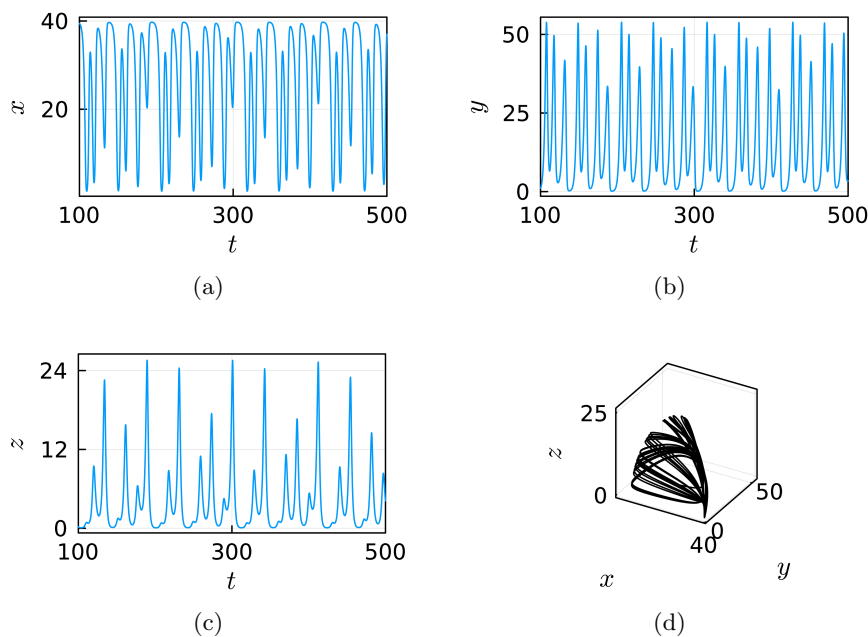


Fig. 1. (a)–(c) The time evaluation of prey, middle predator, and top predator and (d) the phase portrait for model (4) when $\rho_1 = 0, \rho_2 = 0, \tau = 0$, and considering $\alpha_1 = \alpha_2 = \alpha_3 = 1$ shows chaotic dynamics.

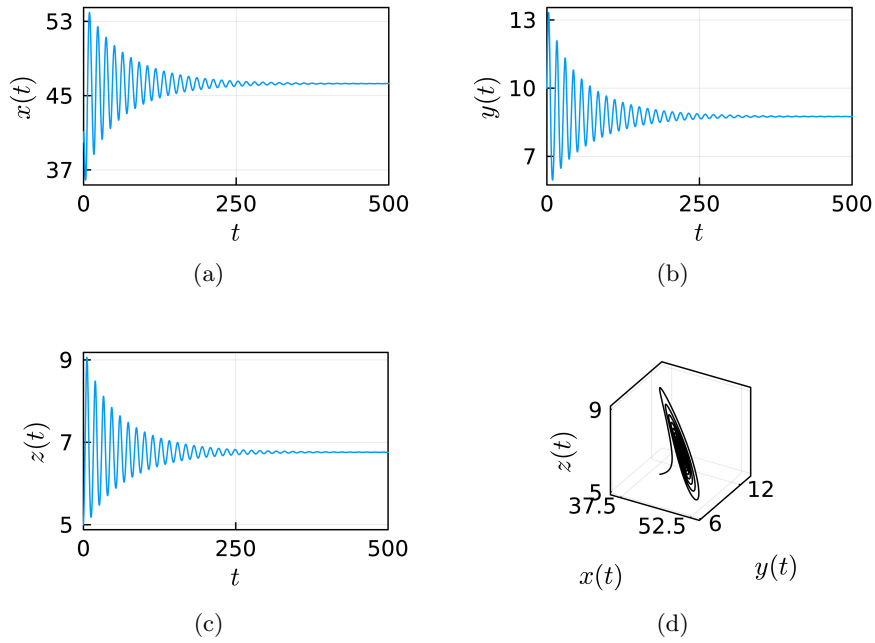


Fig. 2. (a)–(c) The time evaluation of prey, predator, and top predator and (d) the phase portrait for model (4) when $\rho_1 = 0.07$, $\rho_2 = 0.01$, $r_0 = 4$, $\tau = 0$, $\alpha_1 = \alpha_2 = \alpha_3 = 0.9$, and all other parameters are given in (20).

point $E^*(56.4247, 8.75, 7.29287)$, showcasing periodic behavior, as illustrated in Fig. 3.

To illuminate the impact of prey fear in model (4), we construct a bifurcation diagram (Fig. 4). This visual elucidates a transition from periodic to stable dynamics with a gradual reduction in the fear term ρ_1 within the range (0, 0.9).

Furthermore, to underscore the significance of fear’s effect on the middle predator in model (4), we set $\rho_1 = 0.01$ and plot the bifurcation diagram for ρ_2 within the range (0, 0.1) (Fig. 5). This analysis reveals that model (4) experiences stable dynamics via Hopf bifurcation as ρ_2 decreases gradually from the periodic orbit.

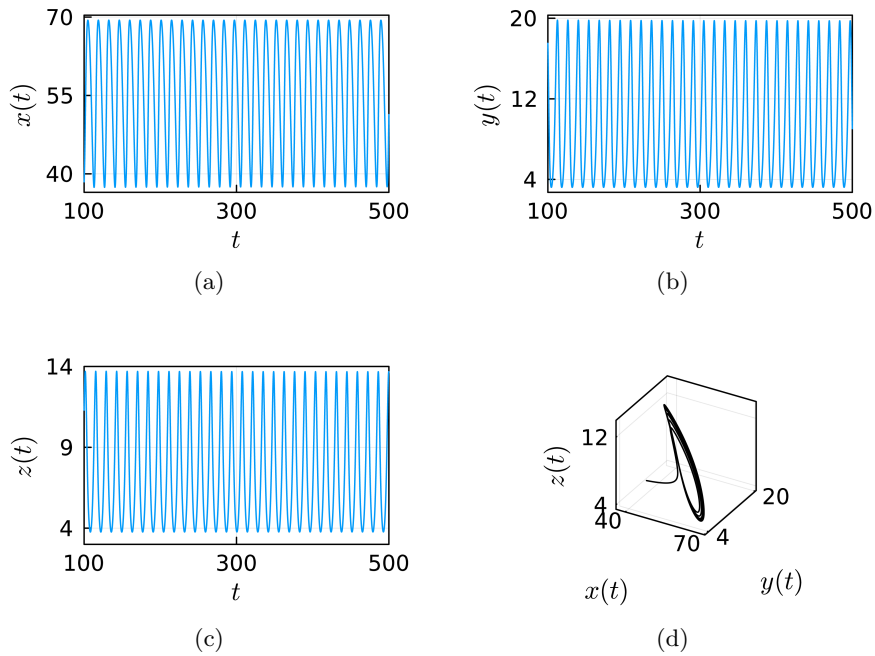


Fig. 3. (a)–(c) The time evaluation of prey, predator, and top predator and (d) the phase portrait for model (4) when $\rho_1 = 0.04$, $\rho_2 = 0.01$, $r_0 = 4$, $\tau = 0$, $\alpha_1 = \alpha_2 = \alpha_3 = 0.9$, and all other parameters are given in (20).

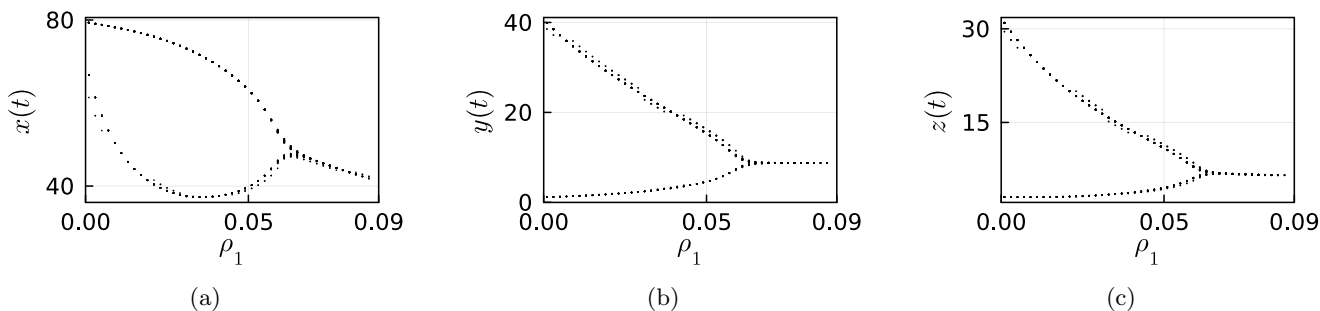


Fig. 4. The bifurcation diagram for model (4) with $\rho_1 \in (0, 0.9)$, $\rho_2 = 0.01$, $r_0 = 4$, $\tau = 0$, $\alpha_1 = \alpha_2 = \alpha_3 = 0.9$, and all other parameters are given in (20).

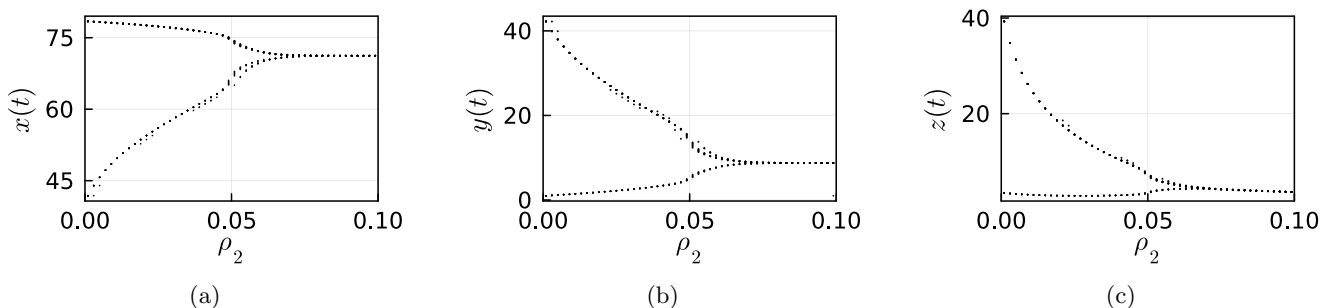


Fig. 5. The bifurcation diagram for model (4) with $\rho_1 = 0.01$, $\rho_2 \in (0, 0.1)$, $r_0 = 4$, $\tau = 0$, $\alpha_1 = \alpha_2 = \alpha_3 = 0.9$, and all other parameters are given in (20).

Moreover, to validate the role of memory effect in model (4)'s complex dynamics, we consider an interior equilibrium point $E^*(71.2083, 8.75, 7.82973)$. The bifurcation diagram with respect to the fractional-order parameter within the range $(0.8, 1.0)$ is illustrated in Fig. 6. It's apparent that model (4) undergoes chaotic dynamics via Hopf bifurcation as α increases. In order to show the sensitivity of model (4), the time plot is depicted in Fig. 7 to show the sensitivity of model with respect to different orders $\alpha = 0.99, 0.97, 0.95, 0.93, 0.91$. For $\alpha = 0.99$, it is chaotic, for $\alpha = 0.97$, it is periodic, and for $\alpha = 0.91$, it is asymptotic behavior. Similarly, time series is plotted in Fig. 8 for different initial conditions, the parameters are taken in

such a way as chaotic. It clearly reveals that the trajectories diverge when time increases, i.e. model (4) is sensitive to the initial conditions.

Subsequently, with $\alpha = 1$, $\rho_1 = 0.1$, $\rho_2 = 0.1$, model (4) converges to an interior equilibrium point $E^*(38.887, 8.75, 2.90712)$. Utilizing (14), we determine $\omega_0 = 0.494991$, and through (15), we ascertain the critical time delay for the birth of Hopf bifurcation as $\tau_0 = 1.24275$. Additionally, the transversality condition (17) holds. The bifurcation diagram in Fig. 9 demonstrates that model (4) undergoes a Hopf bifurcation at the critical time delay $\tau_0 = 1.24275$. As previously stated, an exact periodic solution is not possible for the Caupo-type fractional-order nonlinear system. However, some

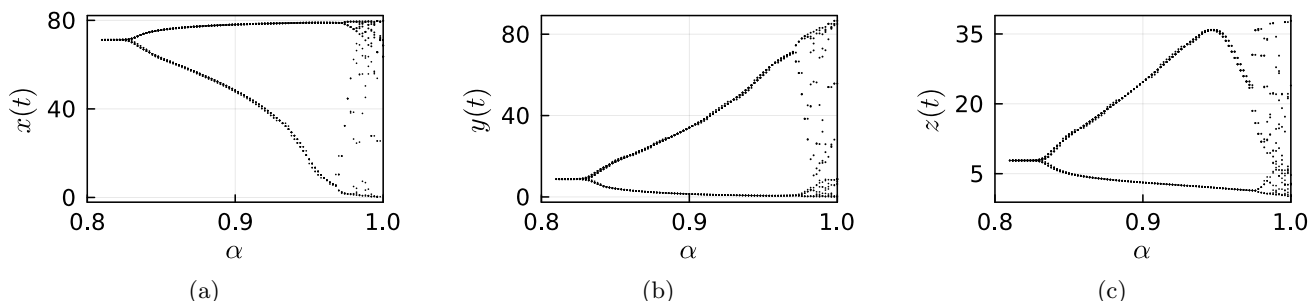


Fig. 6. The bifurcation diagram for model (4) with $\rho_1 = 0.01$, $\rho_2 = 0.01$, $r_0 = 4$, $\tau = 0$, $\alpha_1 = \alpha_2 = \alpha_3 \in (0.8, 1.0)$.

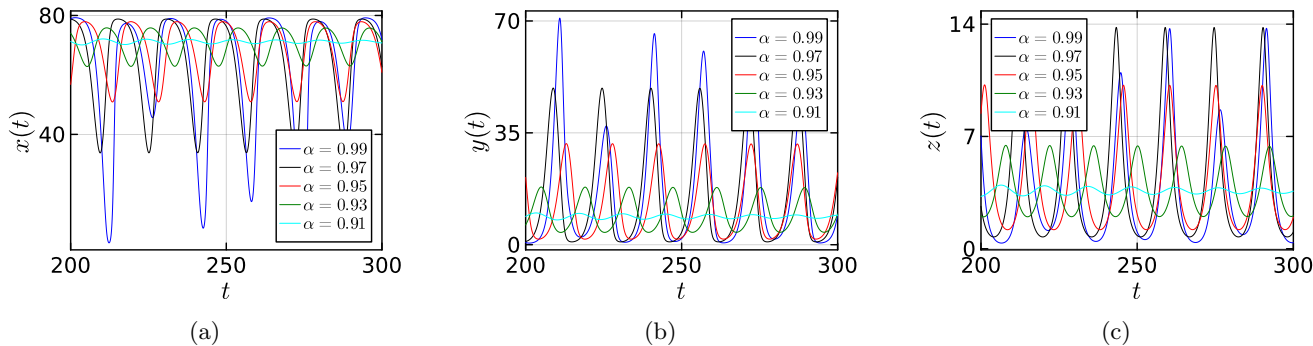


Fig. 7. Sensitivity of model (4) with respect to different order parameters $\alpha = 0.99, 0.97, 0.95, 0.93, 0.91$.

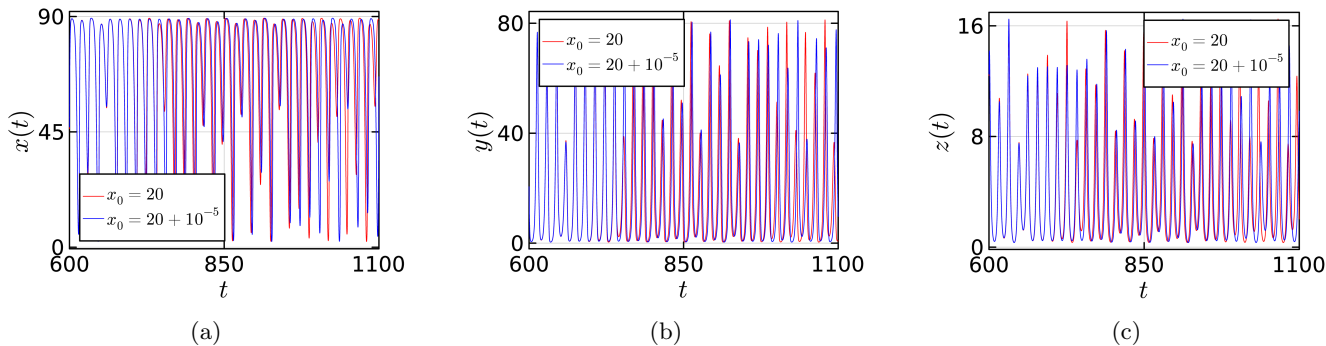


Fig. 8. Sensitivity of model (4) with respect to different initial conditions $x_0 = 20$ (red), $x_0 = 20 + 10^{-5}$ (blue), $y_0 = 10$, and $z_0 = 5$.

recent research articles [Čermák & Nechvátal, 2018; Lin et al., 2017; Wang et al., 2013] indicate the existence of an asymptotically periodic solution for a fractional-order system. In other words, such a solution oscillates close to a periodic function when time increases. However, this periodic function is not a solution to the system.

Lastly, with $\alpha = 1$, $\rho_1 = 0.1$, $\rho_2 = 0.1$, and $\alpha = 0.95$, model (4) converges to an interior equilibrium point $E^*(38.887, 8.75, 2.90712)$. Employing (14), we derive $\omega = 0.492533$, and via (15), we determine the critical time delay for the emergence of Hopf bifurcation as $\tau_0 = 2.38723$. The transversality condition (17) remains valid. The asymptotically

stable time series for $\tau = 2$ is displayed in Fig. 10, and the periodic orbits for $\tau = 3$ are showcased in Fig. 11. Consequently, using Theorem 2, we deduce that the interior equilibrium point of model (4) is asymptotically stable for $\tau \in (0, \tau_0]$ and undergoes a Hopf bifurcation at the critical time delay $\tau_0 = 2.38723$. Next, in order to show the effect of the fractional-order parameter α with fear parameters, the comparison plot is plotted by choosing $\alpha = 1, 0.95$ for the Hopf bifurcation points with respect to ρ_1 and ρ_2 in Fig. 12. It is clear that the stable region expands by choosing the fractional order $\alpha = 0.95$ when compared to $\alpha = 1$.

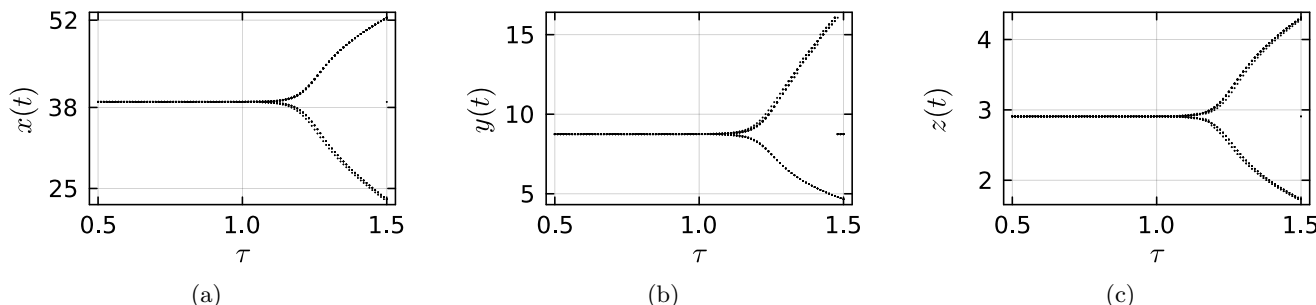


Fig. 9. The bifurcation diagram for model (4) with $\rho_1 = 0.1, \rho_2 = 0.1, r_0 = 4, \alpha_1 = \alpha_2 = \alpha_3 = 1, \tau \in (0.5, 1.5)$.

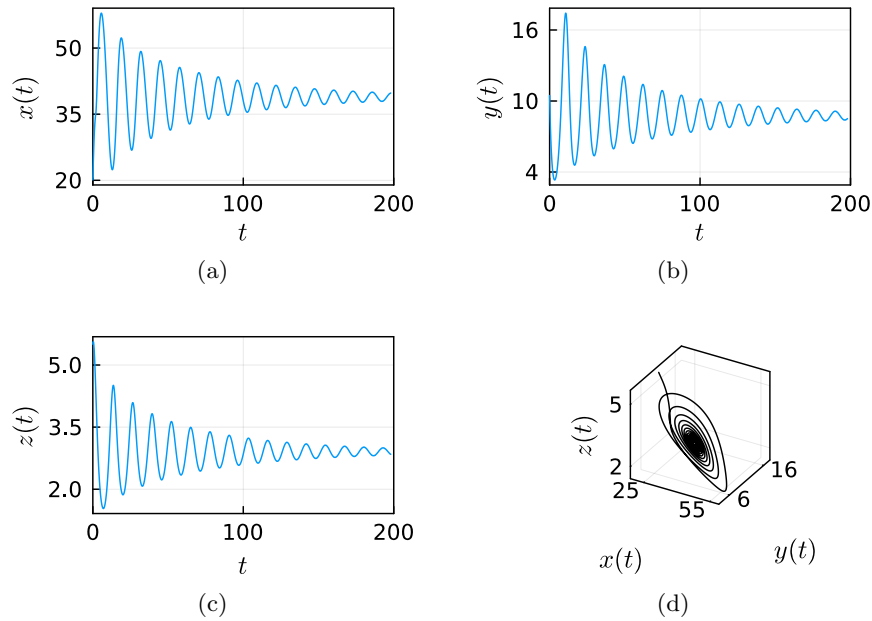


Fig. 10. (a)–(c) The time evaluation of prey, middle predator, and top predator and (d) the phase portrait for model (4) when $\rho_1 = 0.1, \rho_2 = 0.1, r_0 = 4, \tau = 2, \alpha_1 = \alpha_2 = \alpha_3 = 0.95$.

Remark 5.1. The short-term recurrent and robust chaos in the food chain model, which consists of prey, middle predator, and top predator, was studied by [Rai & Upadhyay, 2004]. The consideration of fear effects in prey and middle predators without time delay in the food chain model by [Rai & Upadhyay, 2004] has been explored by the authors in [Kumar & Kumari, 2020]. They reveal that for a low cost of fear, the system remains chaotic,

while an increase in the fear factor leads to stability and further leads to population extinction for a large cost of fear. The authors in [Panday *et al.*, 2020] considered time delay in the fear function in a two-species model and explored how the considered model undergoes Hopf bifurcation for larger time delays. They also demonstrated that time delay in the model induces bistable behavior, i.e. the existence of both stable and unstable

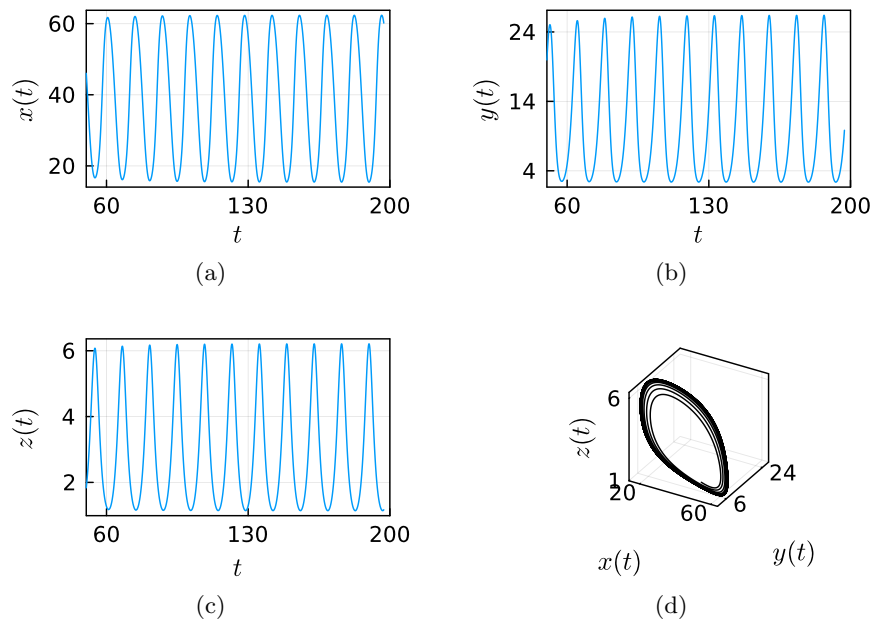


Fig. 11. (a)–(c) The time evaluation of prey, predator, and top predator and (d) the phase portrait for model (4) when $\rho_1 = 0.1, \rho_2 = 0.1, r_0 = 4, \tau = 3, \alpha_1 = \alpha_2 = \alpha_3 = 0.95$.

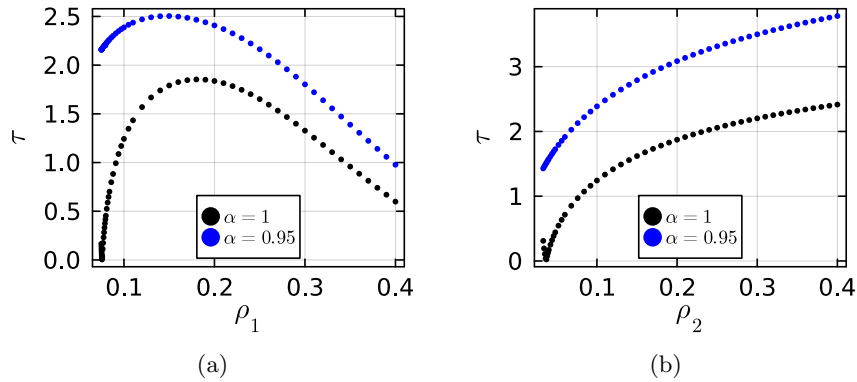


Fig. 12. The Hopf bifurcation points for $\alpha = 1, 0.95$ with respect to ρ_1 and τ in (a) and ρ_2 and τ in (b), respectively. The interior equilibrium point E^* is locally asymptotically stable for the region below the points and periodic for the region above the points.

periodic orbits. Panja [2019] attempted to study stability and Hopf bifurcation by considering fractional order for the model studied by [Rai & Upadhyay, 2004] and showed the existence of periodic and chaotic dynamics with respect to the fractional order. In this study, we explore the effect of considering both fractional order and time delay in the food chain model studied in [Kumar & Kumari, 2020]. We investigate the intricate dynamics in terms of bifurcation behavior with respect to fear, fractional order, and time delay parameters. We showed that the considered model changes from periodic to stable dynamics for larger fear. Further, changes from stable to periodic orbits on increasing the time delay. Also, we revealed the occurrence of period doubling as a route to chaos for the fractional-order parameter.

Remark 5.2. We have varied the fear effects, time delay, and fractional-order parameters and showed how the model is sensitive to the parameter in terms of stability and bifurcation behavior. Also, for the model in a chaotic state, the sensitivity to the initial condition is discussed with the help of how the trajectory moves away for a larger time with small variation in the initial condition. The trajectories of the model simulated above may slightly vary because of numerical error caused to memory effect by both time delay and fractional order. Also, this memory effect causes high computational time for plotting bifurcation diagrams and stimulating models for a larger time.

6. Conclusion

Our study provides detailed insights into the complex dynamics governing predator–prey interactions.

Our research covers a wide range of occurrences, each of which clarifies a distinct aspect of ecological interactions and the underlying processes. Primarily, studying asymptotically stable behavior reveals the remarkable protection and balance attained in food chain ecosystems. This stability behavior explores the long-term survival of a species and explores the complex balancing between prey and predator populations that occurs naturally. It represents both the flexibility of organisms and the complex web of interactions that supports biodiversity. Second, the beginnings of periodic behavior provide evidence for the cyclic fluctuations in the population. We can also find a different meaning for the present results: in many cases, the natural conditions provide useful information. (a) A lot of the periodic phenomena that we can observe in the world. The periodic dynamics in the population fluctuation are one of the dynamic characteristics of the ecosystem. It is due to the seasonal variations and other environmental circumstances. (b) Furthermore, our investigation reveals chaotic dynamics in the population, which is sensitive to the initial condition. The presence of chaos questions the traditional methods for predicting future populations and highlights the need to study probabilistic techniques to understand the population by showing complex behavior. The sensitivity analysis shows how the small fluctuation in the population reacts to the future population trends.

Finding an explanation in some instances could require a deep understanding of the dynamics of model subjected to various environmental situations. In addition, our model gains realism by considering the time delay in the prey’s fear term, which reflects the delay in biological processes.

Zanette *et al.* [2011] experimentally investigated that the fear of predation risk can reduce the reproduction of song sparrow even in the absence of direct killing. The recognition of intricate dynamics highlights the significance of integrating authentic temporal lags into ecological models, offering perspectives on the dynamics of predator–prey interactions in more authentic settings. Finally, investigating fractional-order dynamics unveils the complex interaction between predator–prey dynamics and memory effects. Fractional-order derivatives contribute to our knowledge of ecological processes by capturing the impact of previous conditions on current population dynamics and providing fresh insights into how memory shapes ecosystem dynamics.

Additionally, our model may be widely applied to explain the dynamics of populations in real life in a variety of predator–prey systems. For instance, the model may be applied to simulate the dynamics of predator–prey interactions in aquatic systems, forestry systems, environments with patches, and habitats with spatial organization. Also, it helps in preventing ecological collapse, providing guidelines for conservation policy makers, early identification of ecological crisis, and decision-making process. This type of model approach can also be addressed by machine learning framework by proper training of parameters [Dubois *et al.*, 2020; Wang *et al.*, 2024].

In conclusion, our study offers a comprehensive glimpse into the multifaceted nature of predator–prey interactions, encompassing stability, periodicity, chaos, temporal dynamics, and memory effects. These insights deepen our understanding of ecological dynamics, providing valuable perspectives for conservation efforts, ecosystem management, and the preservation of biodiversity in a rapidly changing world. But this model can be refined further. We can consider the Allee effect and different functional responses to make them more and more realistic.

Acknowledgments

The first author would like to thank SRM IST, Ramapuram, India, for their financial support, vide number SRM/IST-RMP/RI/004.

ORCID

Vinoth Seralan 
<https://orcid.org/0000-0002-4509-9484>

R. Vadivel 
<https://orcid.org/0000-0002-1385-5345>
 Nallappan Gunasekaran 
<https://orcid.org/0000-0003-0375-7917>

References

- Abdelouahab, M. S., Hamri, N. E. & Wang, J. [2012] “Hopf bifurcation and chaos in fractional-order modified hybrid optical system,” *Nonlin. Dyn.* **69**, 275–284.
- Alidousti, J. & Mostafavi Ghahfarokhi, M. [2019] “Dynamical behavior of a fractional three-species food chain model,” *Nonlin. Dyn.* **95**, 1841–1858.
- Al-Raei, M. [2021] “Applying fractional quantum mechanics to systems with electrical screening effects,” *Chaos Solit. Fract.* **150**, 111209.
- Bandyopadhyay, M. & Banerjee, S. [2006] “A stage-structured prey–predator model with discrete time delay,” *Appl. Math. Comput.* **182**, 1385–1398.
- Brauer, F. & Castillo-Chavez, C. [2012] *Mathematical Models in Population Biology and Epidemiology*, Vol. 2 (Springer, NY).
- Britton, N. F. [2003] “Population genetics and evolution,” in *Essential Mathematical Biology* (Springer, NY), pp. 117–146.
- Čermák, J. & Nechvátal, L. [2018] “Local bifurcations and chaos in the fractional Rössler system,” *Int. J. Bifurcation and Chaos* **28**, 1850098.
- Creel, S., Christianson, D., Liley, S. & Winnie Jr., J. A. [2007] “Predation risk affects reproductive physiology and demography of elk,” *Science* **315**, 960.
- Cresswell, W. [2011] “Predation in bird populations,” *J. Ornithol.* **152**, 251–263.
- Cui, W. & Zhao, Y. [2024] “Bifurcation analysis of a predator–prey model with alternative prey and prey refuges,” *Int. J. Bifurcation and Chaos* **34**, 2450021.
- Danca, M. F. [2021] “Matlab code for Lyapunov exponents of fractional-order systems, part II: The non-commensurate case,” *Int. J. Bifurcation and Chaos* **31**, 2150187.
- Das, M. & Samanta, G. P. [2020] “A delayed fractional order food chain model with fear effect and prey refuge,” *Math. Comput. Simul.* **178**, 218–245.
- Du, M., Wang, Z. & Hu, H. [2013] “Measuring memory with the order of fractional derivative,” *Sci. Rep.* **3**, 3431.
- Dubey, B. & Kumar, A. [2019] “Dynamics of prey–predator model with stage structure in prey including maturation and gestation delays,” *Nonlin. Dyn.* **96**, 2653–2679.
- Dubois, P., Gomez, T., Planckaert, L. & Perret, L. [2020] “Data-driven predictions of the Lorenz system,” *Physica D* **408**, 132495.

- Elsadany, A. A. & Matouk, A. E. [2015] “Dynamical behaviors of fractional-order Lotka–Volterra predator–prey model and its discretization,” *J. Appl. Math. Comput.* **49**, 269–283.
- Fan, Y., Huang, X., Wang, Z. & Li, Y. [2018] “Global dissipativity and quasi-synchronization of asynchronous updating fractional-order memristor-based neural networks via interval matrix method,” *J. Franklin Inst.* **355**, 5998–6025.
- Hethcote, H. W. [2000] “The mathematics of infectious diseases,” *SIAM Rev.* **42**, 599–653.
- Huang, C., Song, X., Fang, B., Xiao, M. & Cao, J. [2018] “Modeling, analysis and bifurcation control of a delayed fractional-order predator–prey model,” *Int. J. Bifurcation and Chaos* **28**, 1850117.
- Huang, X., Chen, L., Xia, Y. & Chen, F. [2023] “Dynamical analysis of a predator–prey model with additive Allee effect and migration,” *Int. J. Bifurcation and Chaos* **33**, 2350179.
- Islam, M. S., Sk, N. & Sarwardi, S. [2023] “Deterministic and stochastic study of an eco-epidemic predator–prey model with nonlinear prey refuge and predator harvesting,” *Eur. Phys. J. Plus* **138**, 851.
- Kuang, Y. [1993] *Delay Differential Equations* (Elsevier, NY).
- Kumar, V. & Kumari, N. [2020] “Controlling chaos in three species food chain model with fear effect,” *AIMS Math.* **5**, 828–842.
- Kumbhakar, R., Hossain, M. & Pal, N. [2024] “Dynamics of a two-prey one-predator model with fear and group defense: A study in parameter planes,” *Chaos Solit. Fract.* **179**, 114449.
- Laskin, N. [2000] “Fractional quantum mechanics,” *Phys. Rev. E* **62**, 3135.
- Laundré, J. W., Hernández, L. & Altendorf, K. B. [2001] “Wolves, elk, and bison: Reestablishing the ‘landscape of fear’ in Yellowstone National Park, USA,” *Can. J. Zool.* **79**, 1401–1409.
- Lin, X., Liao, B. & Zeng, C. [2017] “The onset of chaos via asymptotically period-doubling cascade in fractional order Lorenz system,” *Int. J. Bifurcation and Chaos* **27**, 1750207.
- Naik, P. A., Zu, J. & Owolabi, K. M. [2020] “Modeling the mechanics of viral kinetics under immune control during primary infection of HIV-1 with treatment in fractional order,” *Physica A* **545**, 123816.
- Neuhauser, C. [2001] “Mathematical challenges in spatial ecology,” *Notices AMS* **48**, 1304–1314.
- Pal, S., Pal, N., Samanta, S. & Chattopadhyay, J. [2019] “Fear effect in prey and hunting cooperation among predators in a Leslie–Gower model,” *Math. Biosci. Eng.* **16**, 5146.
- Pal, S., Karmakar, S., Pal, S., Pal, N., Misra, A. K. & Chattopadhyay, J. [2024] “Impact of fear and group defense on the dynamics of a predator–prey system,” *Int. J. Bifurcation and Chaos* **34**, 2450019.
- Panday, P., Samanta, S., Pal, N. & Chattopadhyay, J. [2020] “Delay induced multiple stability switch and chaos in a predator–prey model with fear effect,” *Math. Comput. Simul.* **172**, 134–158.
- Panja, P. [2019] “Stability and dynamics of a fractional-order three-species predator–prey model,” *Theory Biosci.* **138**, 251–259.
- Podlubny, I. [1998] *Fractional Differential Equations* (Academic Press, NY).
- Qi, H. & Zhao, W. [2022] “Stability and bifurcation analysis of a fractional-order food chain model with two time delays,” *J. Math.* **2022**, 5313931.
- Rai, V. & Upadhyay, R. K. [2004] “Chaotic population dynamics and biology of the top-predator,” *Chaos Solit. Fract.* **21**, 1195–1204.
- Rasooli Berardehi, Z., Zhang, C., Taheri, M., Roohi, M. & Khooban, M. H. [2023] “A fuzzy control strategy to synchronize fractional-order nonlinear systems including input saturation,” *Int. J. Intell. Syst.* **2023**, 1550256.
- Ripple, W. J. & Beschta, R. L. [2004] “Wolves and the ecology of fear: Can predation risk structure ecosystems?” *BioScience* **54**, 755–766.
- Roohi, M., Mirzajani, S. & Basse-O’Connor, A. [2023a] “A no-chatter single-input finite-time PID sliding mode control technique for stabilization of a class of 4D chaotic fractional-order laser systems,” *Mathematics* **11**, 4463.
- Roohi, M., Zhang, C., Taheri, M. & Basse-O’Connor, A. [2023b] “Synchronization of fractional-order delayed neural networks using dynamic-free adaptive sliding mode control,” *Fractal Fract.* **7**, 682.
- Sabarathinam, S., Papov, V., Wang, Z.-P., Vadivel, R. & Gunasekaran, N. [2023] “Dynamics analysis and fractional-order nonlinearity system via memristor-based Chua oscillator,” *Pramana* **97**, 107.
- Taheri, M., Chen, Y., Zhang, C., Berardehi, Z. R., Roohi, M. & Khooban, M. H. [2023] “A finite-time sliding mode control technique for synchronization chaotic fractional-order laser systems with application on encryption of color images,” *Optik* **285**, 170948.
- Tavazoei, M. S. & Haeri, M. [2009] “A proof for non existence of periodic solutions in time invariant fractional order systems,” *Automatica* **45**, 1886–1890.
- Tavazoei, M. S., Haeri, M., Attari, M., Bolouki, S. & Siami, M. [2009] “More details on analysis of fractional-order Van der Pol oscillator,” *J. Vib. Control* **15**, 803–819.
- Tavazoei, M. S. [2010] “A note on fractional-order derivatives of periodic functions,” *Automatica* **46**, 945–948.
- Upadhyay, R. K. & Agrawal, R. [2016] “Dynamics and responses of a predator–prey system with competitive interference and time delay,” *Nonlin. Dyn.* **83**, 821–837.

- Vinoth, S., Sivasamy, R., Sathiyathan, K., Rajchakit, G., Hammachukiattikul, P., Vadivel, R. & Gunasekaran, N. [2021a] “Dynamical analysis of a delayed food chain model with additive Allee effect,” *Adv. Diff. Eqs.* **2021**, 54.
- Vinoth, S., Sivasamy, R., Sathiyathan, K., Unyong, B., Rajchakit, G., Vadivel, R. & Gunasekaran, N. [2021b] “The dynamics of a Leslie type predator–prey model with fear and Allee effect,” *Adv. Diff. Eqs.* **2021**, 338.
- Vinoth, S., Vadivel, R., Hu, N. T., Chen, C. S. & Gunasekaran, N. [2023] “Bifurcation analysis in a harvested modified Leslie–Gower model incorporated with the fear factor and prey refuge,” *Mathematics* **11**, 3118.
- Wang, J., Fec, M., Zhou, Y. *et al.* [2013] “Nonexistence of periodic solutions and asymptotically periodic solutions for fractional differential equations,” *Commun. Nonlin. Sci. Numer. Simul.* **18**, 246–256.
- Wang, W., Wang, G., Ying, J., Liu, G. & Liang, Y. [2022] “Dynamics of a fractional-order voltage-controlled locally active memristor,” *Pramana* **96**, 109.
- Wang, X., Feng, J., Xu, Y. & Kurths, J. [2024] “Deep learning-based state prediction of the Lorenz system with control parameters,” *Chaos* **34**, 033108.
- Xiao, Y. & Chen, L. [2001] “Modeling and analysis of a predator–prey model with disease in the prey,” *Math. Biosci.* **171**, 59–82.
- Xu, R. [2011] “Global dynamics of a predator–prey model with time delay and stage structure for the prey,” *Nonlin. Anal.: Real World Appl.* **12**, 2151–2162.
- Yazdani, M. & Salarieh, H. [2011] “On the existence of periodic solutions in time-invariant fractional order systems,” *Automatica* **47**, 1834–1837.
- Zanette, L. Y., White, A. F., Allen, M. C. & Clinchy, M. [2011] “Perceived predation risk reduces the number of offspring songbirds produce per year,” *Science* **334**, 1398–1401.
- Zhao, L., Huang, C. & Cao, J. [2021] “Dynamics of fractional-order predator–prey model incorporating two delays,” *Fractals* **29**, 2150014.

Appendix A

For the fear function $f(\rho, v) = \frac{1}{1+\rho v}$, the following assumptions hold:

- (1) $f(0, v) = 1$: if there is no anti-predator behaviors, then the birth rate of prey remains unchanged.
- (2) $f(\rho, 0) = 1$: there is no reduction in prey population in the absence of anti-predator behaviors.
- (3) $\lim_{\rho \rightarrow \infty} f(\rho, v) = 0$: if anti-predator behaviors are very large, the prey reproduction declines and becomes zero.
- (4) $\lim_{v \rightarrow \infty} f(\rho, v) = 0$: if $\rho > 0$ and predator population is high, then the prey reproduction declines and becomes zero.
- (5) $\frac{\partial f(\rho, v)}{\partial \rho} < 0$: the reproduction of prey decreases with the increase of anti-predator behaviors.
- (6) $\frac{\partial f(\rho, v)}{\partial v} < 0$: the reproduction of prey decreases with the increase of predator populations.